# Influence of non-singular higher order terms on the stress field of thin welded lap joints and small inclined cracks in plates

F. Berto, P. Lazzarin
*University of Padova, Department of Management and Engineering,Stradella S.Nicola 3, 36100 Vicenza (Italy)*
*plazzarin@gest.unipd.it*

C.J. Christopher, M.N. James
*Faculty of Science and Technology, University of Plymouth, Drake Circus, Plymouth, PL4 8AA, United Kingdom*
*M.James@plymouth.ac.uk*

**ABSTRACT.** In stress analysis of cracked plates, alongside the stress intensity factor which quantifies the singular stress component perpendicular to the crack plane, the role played in crack growth by the constant term parallel to the crack plane, called the T-stress, has been widely investigated by many researchers. There are, however, cases of practical interest where the influence on the stress field of the higher order terms in the series expansion for the crack tip stress field, is not negligible. The main aim of the present investigation is to present and apply a set of equations able to describe more accurately the stress components for those cases where the mode I and mode II stress intensity factors used in combination with the T-stress are unable to characterise with sufficient precision the complete stress field ahead the crack tip. The starting point is represented by the Williams' solution (Williams, 1957) where stresses as expressed in terms of a power series. An example is investigated of a thin-thickness welded lap joint characterized by various joint width to thickness ratios, in the range of $d/t$ ranging from 0.5 to 5. The present paper indicates that the local stresses as well as the strain energy averaged over a control volume which embraces the slip tip, can be evaluated with satisfactory precision only by taking into account a further four terms besides $K_I$, $K_{II}$ and T-stress.

**KEYWORDS.** Crack; Stress intensity factors; *T*-stress; Higher order terms; Strain energy.

## INTRODUCTION

As a part of a more general two-dimensional study on sharp V-notches in plates, the specific case of a zero angle V-notch, or crack, was carried out by Williams [1] to supplement previous results by Inglis (1913), Griffith (1921), and Westergaard (1939). For the crack case Williams demonstrated that the stress function can be expressed as a series expansion, being the coefficients of each term undetermined and depending on the loading conditions. Williams also underlined that for practical cases when the plate has finite dimensions, higher order eigenfunctions should be used to determine a solution in the large. The stress associated with the symmetric and skew-symmetric singular terms in combination with the constant term were finally presented by Williams, neglecting the other terms proportional to $r^{1/2}$, $r$, $r^{3/2}$. Today, after Larsson and Carlsson and Rice, the constant stress term is commonly called T-stress [2, 3]. By using a

boundary collocation technique, a procedure to determine mode I and mode II stress intensity factors was proposed by Gross and Mendelson [4]. The collocation technique was later used also by Carpenter [5] to determine the coefficients associated both to singular and non-singular stress terms. Carpenter presented some examples where the main aim was to handle the complex coefficients of higher order terms.
However, after Williams up to now, classical theories of fracture mechanics generally assume that the near-crack-tip stresses can be characterized by the stress intensity factors but extensive studies in the last two decades have shown that also the T-stress is important for describing the states of stress and strain near the crack tip [6-10].
The role of the *T*-stress in brittle fracture for linear elastic materials has been emphasized by Ayatollahi *et al.* [6] who proposed a modified Erdogan-Sih's criterion (Erdogan, Sih, 1963). Their generalized maximum tensile stress criterion is based on the mode I and II stress intensity factors, $K_I$ and $K_{II}$, the *T*-stress and a fracture process zone parameter, $r_c$..
Several closed form solutions of T-stress in plane elasticity crack problems in an infinite plate are investigated using the complex potential theory [7]. A rigorous derivation for T-stress in line crack problem is presented by Chen *et al.* (2010). Similar to the edge crack case, this paper provides the T-stress dependence on loading with the Dirac delta function property [11].Dealing with mixed mode loading a particular weight function method is used to determine the stress intensity factors (SIFs) and *T* -stresses for offset double edge cracked plates under mixed mode loading [12].
Beyond the T-stress, the problem related to the different role played by the higher order terms remain open. Ramesh et al. [13, 14] presented an over-deterministic least squares technique to evaluate the mixed-mode multi-parameter stress field by photoelasticity underlining the fact that the use of a multi-parametric representation is not just an a academic curiosity but a necessity in some cases of engineering interest. This fact is underlined also by Ayatollahi and Nejati [15] who provided a specific algorithm for a fast determinations of the unknown parameters. A method for the direct determination of SIF and higher order terms by a hybrid crack element has been developed in the past also by Xiao et al. [16] proving the versatility and accuracy of the element for pure mode I problems and for mode II and mixed mode cracks. An overview of a hybrid crack element and determination of its complete displacement field has been carried out by Xiao and Karihaloo [17].
A novel mathematical model of the stresses around the tip of a fatigue crack, which Includes the T-stress and considers the effects of plasticity through an analysis of their shielding effects on the applied elastic field was developed by Christopher *et al.* [8, 9]. The ability of the model to characterize plasticity-induced effects of cyclic loading and on the elastic stress fields was demonstrated using full field photoelasticity. The effects due to overloads have been also discussed [10]. The model can be seen as a modified linear elastic approach, to be applied outside the zone where nonlinear effects are prevailing. Two logarithmic terms are added to the Williams' solution and three new stress intensity factors $K_F$, $K_R$ and $K_S$ are proposed to quantify shielding effects ahead of the crack tip and on its back.
The present Authors have been recently interested in the fatigue strength of welded lap joints and they have paid particular attention to thin plates characterized by a thickness equal or lower than 5 mm [18, 19]. In that study, the T-stress was considered together with $K_I$ and $K_{II}$ to describe the stress field. The closed form expressions involving only these three parameters was found to be inadequate to accurately describe the actual stress fields in thin welded lap joints as well as the mean value of the strain energy density on a control volume embracing the slit tip.
Decreasing the plate thickness of the welded joint, the zone controlled by the first order terms became smaller than the characteristic control volume of the welded material. The effect of the higher order terms will be object of the present contribution and a demarcation line between linear elastic and elastic-plastic analyses will be drawn on the basis of the local strain energy density creating also a bridging with the recent model proposed by Christopher et al. [8, 9].

## ANALYTICAL BACKGROUND

Following Williams' approach a generic term of the stress function expressed as a series expansion can be written in the following form [1]:

$$\chi(r,\theta) = r^{(n/2)+1}\left\{a_i\left[\sin\left(\frac{n}{2}-1\right)\theta - \frac{n-2}{n+2}\sin\left(\frac{n}{2}+1\right)\theta\right] + a_j\left[\cos\left(\frac{n}{2}-1\right)\theta - \cos\left(\frac{n}{2}+1\right)\theta\right]\right\} \quad (1)$$

By explicitly writing the terms of the series (1), the stress function becomes:

$$\chi(\mathrm{r},\theta)=-\frac{4}{3}\mathrm{r}^{3/2}\left(\sin\frac{\theta}{2}\right)^2\left(a_1\sin\frac{\theta}{2}-3a_2\cos\frac{\theta}{2}\right)+2a_3\mathrm{r}^2\left(\sin\theta\right)^2+$$
$$+\mathrm{r}^{5/2}\left[\frac{4}{5}a_4\left(3+2\cos\theta\right)\left(\sin\frac{\theta}{2}\right)^3+a_5\left(\cos\frac{\theta}{2}-\cos\frac{5}{2}\theta\right)\right]+$$
$$+\frac{4}{3}\mathrm{r}^3\left(\sin\theta\right)^2\left[a_6\sin\theta+3a_7\cos\theta\right]+$$
$$+\mathrm{r}^{7/2}\left[a_8\left(\sin\frac{3}{2}\theta-\frac{3}{7}\sin\frac{7}{2}\theta\right)+a_9\left(\cos\frac{3}{2}\theta-\cos\frac{7}{2}\theta\right)\right]+ \quad (2)$$
$$+2\mathrm{r}^4\left(\sin\theta\right)^2\left[a_{10}\sin2\theta+a_{11}\left(1+2\cos2\theta\right)\right]+$$
$$+\mathrm{r}^{9/2}\left[a_{12}\left(\sin\frac{5}{2}\theta-\frac{5}{9}\sin\frac{9}{2}\theta\right)+a_{13}\left(\cos\frac{5}{2}\theta-\cos\frac{9}{2}\theta\right)\right]$$

Here $a_1$, $a_2$, $a_3$, $a_4$, etc. are the undetermined parameters whereas $\theta$ is the angle shown in figure 1 (with $\theta=\psi+\pi$. As well known, there is a precise link between the three first coefficients of eq.(2) which control the stress intensity factors ($K_I$ $K_{II}$) and the T-stress according to the expressions:

$$a_1=K_I/\sqrt{2\pi}\quad a_2=K_{II}/\sqrt{2\pi}\quad a_3=T/4 \quad (3)$$

In the contribution by Williams (1957), although fundamental and pioneering, some typos were present where higher order terms were presented by splitting into even and odd parts the initial stress function (ibid. Eqs 8 and 9). In order to avoid misunderstandings, all stress components are determined here by directly using the stress function approach, according to which:

$$\sigma_{rr}\left(\mathrm{r},\psi\right)=\frac{1}{r^2}\partial_\psi^2\chi+\frac{1}{r}\partial_r\chi$$
$$\sigma_{\psi\psi}\left(\mathrm{r},\psi\right)=\partial_r^2\chi \quad (4)$$
$$\sigma_{r\psi}\left(\mathrm{r},\psi\right)=-\frac{1}{r}\partial_\psi\partial_r\chi+\frac{1}{r^2}\partial_\psi\chi$$

The generic n-th terms of the stress distributions are then as follows:

$$\sigma_{rr}\left(\mathrm{r},\psi,\mathrm{n}\right)=\frac{n}{4}r^{n/2-1}\left[a_i(n-2)\sin\left(\frac{n+2}{2}(\psi+\pi)\right)+a_j(n+2)\cos\left(\frac{n+2}{2}(\psi+\pi)\right)+\right.$$
$$\left.-a_i\left(n-6\right)\sin\left(\frac{n-2}{2}(\psi+\pi)\right)-a_j\left(n-6\right)\cos\left(\frac{n-2}{2}(\psi+\pi)\right)\right] \quad (5a)$$

$$\sigma_{\psi\psi}\left(\mathrm{r},\psi,\mathrm{n}\right)=\frac{n}{4}r^{n/2-1}\left[a_i(n+2)\sin\left(\frac{n-2}{2}(\psi+\pi)\right)-a_i(n-2)\sin\left(\frac{n+2}{2}(\psi+\pi)\right)+\right.$$
$$\left.+a_j\left(n+2\right)\cos\left(\frac{n-2}{2}(\psi+\pi)\right)-a_j\left(n+2\right)\cos\left(\frac{n+2}{2}(\psi+\pi)\right)\right] \quad (5b)$$

$$\sigma_{r\psi}\left(\mathrm{r},\psi,\mathrm{n}\right)=-\frac{n}{4}r^{n/2-1}\left[a_i(n-2)\cos\left(\frac{n-2}{2}(\psi+\pi)\right)-a_i(n-2)\cos\left(\frac{n+2}{2}(\psi+\pi)\right)+\right.$$
$$\left.-a_j(n-2)\sin\left(\frac{n-2}{2}(\psi+\pi)\right)+a_j(n+2)\sin\left(\frac{n+2}{2}(\psi+\pi)\right)\right] \quad (5c)$$

For n=1 the subscripts are i=1 and j=2; for n=2 we have here only j=3 (because the correspondent terms containing $a_i$ disappear). Finally, for n>2, the subscripts are i=2n − 2 and j=2n−1.
Equations 5a-c are given also in [13, 14] where they are splitted into symmetric and skew-symmetric terms. Analogous equations are given also in [15-17] with inclusion of the terms linked to the rigid translation of the slit tip and the rigid body rotation with respect to the same point.
By considering the first 13 parameters ($a_1$,…, $a_{13}$) of the Williams' series, the stress field can be explicitly derived:

$$\begin{aligned}\sigma_{rr} = {} & \frac{1}{4r^{1/2}}\left(a_1\cos\frac{3}{2}\psi - 5a_1\cos\frac{\psi}{2} + 3a_2\sin\frac{3}{2}\psi - 5a_2\sin\frac{\psi}{2}\right) + 4a_3\left(\cos\psi\right)^2 + \\ & + \frac{r^{1/2}}{4}\left(9a_4\cos\frac{\psi}{2} + 3a_4\cos\frac{5}{2}\psi - 9a_5\sin\frac{\psi}{2} - 15a_5\sin\frac{5}{2}\psi\right) + \\ & + r\left(-8a_6\left(\cos\psi\right)^2\sin\psi - 2a_7\cos\psi - 6a_7\cos 3\psi\right) + \\ & + \frac{r^{3/2}}{4}\left(-5a_8\cos\frac{3}{2}\psi - 15a_8\cos\frac{7}{2}\psi + 5a_9\sin\frac{3}{2}\psi + 35a_9\sin\frac{7}{2}\psi\right) + \\ & + r^2\left(6a_{10}\sin 4\psi + 12a_{11}\cos 4\psi\right) + \\ & + \frac{r^{5/2}}{4}\left(-7a_{12}\cos\frac{5}{2}\psi + 35a_{12}\cos\frac{9}{2}\psi + 7a_{13}\sin\frac{5}{2}\psi - 63a_{13}\sin\frac{9}{2}\psi\right)\end{aligned} \tag{6a}$$

$$\begin{aligned}\sigma_{\psi\psi} = {} & \frac{1}{r^{1/2}}\left(-a_1\left(\cos\frac{\psi}{2}\right)^3 - 3a_2\sin\frac{\psi}{2}\left(\cos\frac{\psi}{2}\right)^2\right) + 4a_3\left(\sin\psi\right)^2 + \\ & + r^{1/2}\left(9a_4\left(\cos\frac{\psi}{2}\right)^3 - 6a_4\cos\psi\left(\cos\frac{\psi}{2}\right)^3 - \frac{15}{4}a_5\sin\frac{\psi}{2} + \frac{15}{4}a_5\sin\frac{5}{2}\psi\right) + \\ & + r\left(-8a_6\left(\sin\psi\right)^3 - 24a_7\left(\sin\psi\right)^2\cos\psi\right) + \\ & + \frac{r^{3/2}}{4}\left(-35a_8\cos\frac{3}{2}\psi + 15a_8\cos\frac{7}{2}\psi + 35a_9\sin\frac{3}{2}\psi - 35a_9\sin\frac{7}{2}\psi\right) + \\ & + r^2\left(24a_{10}\left(\sin\psi\right)^2\sin 2\psi + 24a_{11}\left(\sin\psi\right)^2 + 48a_{11}\left(\sin\psi\right)^2\cos 2\psi\right) + \\ & + \frac{r^{5/2}}{4}\left(63a_{12}\cos\frac{5}{2}\psi - 35a_{12}\cos\frac{9}{2}\psi - 63a_{13}\sin\frac{5}{2}\psi + 63a_{13}\sin\frac{9}{2}\psi\right)\end{aligned} \tag{6b}$$

Along the bisector line the stress components turn out to be:

$$\sigma_{rr} = -\frac{a_1}{r^{1/2}} + 4a_3 + 3r^{1/2}a_4 - 8a_7 r - 5a_8 r^{3/2} + 12a_{11}r^2 + 7a_{12}r^{5/2} \tag{7a}$$

$$\sigma_{\psi\psi} = -\frac{a_1}{r^{1/2}} + 3r^{1/2}a_4 - 5a_8 r^{3/2} + 7a_{12}r^{5/2} \tag{7b}$$

$$\sigma_{r\psi} = \frac{a_2}{r^{1/2}} - 3r^{1/2}a_5 + 5a_9 r^{3/2} - 7a_{13}r^{5/2} \tag{7c}$$

Along the direction $\psi = \pi$, the unique non vanishing stress component is the radial stress $\sigma_{rr}$:

$$\sigma_{rr} = -\frac{2a_2}{r^{1/2}} + 4a_3 - 6r^{1/2}a_5 + 8a_7 r - 10a_9 r^{3/2} + 12a_{11}r^2 - 14a_{13}r^{5/2} \tag{8}$$

It is important to underline that, for the welded lap joint shown in Fig. 1, the polar angle $\psi$ providing the maximum tangential stress $\sigma_{\psi\psi}$ and the corresponding provisional crack propagation angle is close to $\pi/2$ due to the high contribution due to mode II in this kind of geometry. In the light of this consideration the expression of the stress components in that direction are of particular interest.
Along the direction $\psi = \pi/2$ we have:

$$\sigma_{rr} = -\frac{3a_1}{2\sqrt{2}r^{1/2}} - \frac{a_2}{2\sqrt{2}r^{1/2}} + \frac{3a_4}{2\sqrt{2}}r^{1/2} + \frac{3a_5}{2\sqrt{2}}r^{1/2} - \frac{5a_8}{2\sqrt{2}}r^{3/2} + \\ -\frac{15a_9}{2\sqrt{2}}r^{3/2} + 12a_{11}r^2 + \frac{21a_{12}}{2\sqrt{2}}r^{5/2} - \frac{35a_{13}}{2\sqrt{2}}r^{5/2} \tag{9a}$$

$$\sigma_{\psi\psi} = -\frac{a_1}{2\sqrt{2}r^{1/2}} - \frac{3a_2}{2\sqrt{2}r^{1/2}} + 4a_3 + \frac{9a_4}{2\sqrt{2}}r^{1/2} - \frac{15a_5}{2\sqrt{2}}r^{1/2} - 8ra_6 + \\ +\frac{25a_8}{2\sqrt{2}}r^{3/2} + \frac{35a_9}{2\sqrt{2}}r^{3/2} - 24a_{11}r^2 - \frac{49a_{12}}{2\sqrt{2}}r^{5/2} + \frac{63a_{13}}{2\sqrt{2}}r^{5/2} \tag{9b}$$

$$\sigma_{r\psi} = -\frac{a_1}{2\sqrt{2}r^{1/2}} - \frac{a_2}{2\sqrt{2}r^{1/2}} + \frac{3a_4}{2\sqrt{2}}r^{1/2} + \frac{9a_5}{2\sqrt{2}}r^{1/2} - 8ra_7 - \frac{15a_8}{2\sqrt{2}}r^{3/2} + \\ +\frac{25a_9}{2\sqrt{2}}r^{3/2} + 12a_{10}r^2 - \frac{35a_{12}}{2\sqrt{2}}r^{5/2} - \frac{49a_{13}}{2\sqrt{2}}r^{5/2} \tag{9c}$$

## STRESS FIELD AT THE SLIT TIP OF A THIN WELDED LAP JOINT

The geometry of lap joint subjected to tensile-shear loading is shown in Fig. 1. The initial value of the thickness is t=1 mm, whereas the ratio d/t ranges from 0.5 to 5.0. The applied load F results in a membrane nominal stress F/t = 10 MPa. On the slit edge side of point O, the membrane stress (10 MPa) and the bending stress (30 MPa) are superimposed, resulting in a total nominal stress of 40 MPa.
Parameters $a_1$, $a_2$, $a_3$ are derived directly from $K_I$, $K_{II}$ and the T-stress respectively by means of Eq. (3). The original values of $K_I$, $K_{II}$ and T stress match those reported in Lazzarin et al. [18]. The parameters $a_4$, $a_5$, $a_7$ are set by imposing the condition that numerical values of the stress components $\sigma_{\psi\psi}$, $\sigma_{rr}$, $\sigma_{r\psi}$ coincide with theoretical prediction along the slit ligament far from the tip. This distance varied as a function of the ratio d/t.
Dealing with the ratio d/t=1, $a_4$ and $a_5$ have been directly determined along the bisector line by a condition on $\sigma_{\psi\psi}$ and $\sigma_{r\psi}$ at a distance r=0.1 mm and r=0.4 mm, respectively. The parameter $a_7$ has been then derived by a condition on $\sigma_{\rho\rho}$ at r = 0.4 mm and $\psi$=0; finally the parameter $a_6$ has been obtained by a condition on $\sigma_{\psi\psi}$ at r = 0.1 mm along the direction $\psi=\pi/2$.
Stress components along the slit ligament as determined from the finite element model with t=1 mm and d/t=1 are shown in Fig. 2. The stress components are plotted along the direction $\psi$=0° over a distance less than or equal to 1.0 mm. The FE results are compared with Eqs (7a-c) along the slit bisector line considering the first seven parameters, from $a_1$ to $a_7$, see Tab. 1. The plot of $\sigma_{rr}$ along the direction $\psi$=180° is also documented as well as the theoretical stress fields limited to $K_I$, $K_{II}$ and the T-stress, which are reported for comparison.

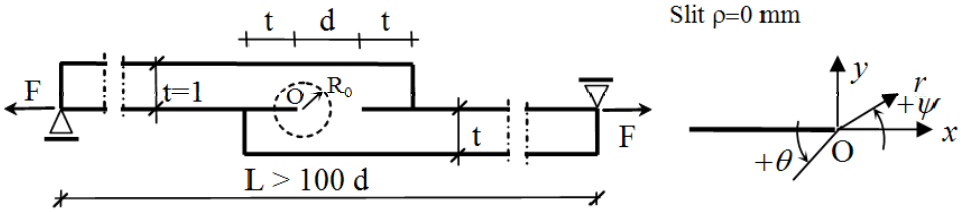


Figure 1: Geometry of the welded lap joint.

The figure shows that the agreement between analytical frame and numerical results is satisfactory only by using of a multi-parameter stress field equation. It is important to note that the parameters $a_5$ and $a_7$ in Eq.( 8) for the radial stress component at $\psi=180°$ were determined by involving parameters set in the other directions as explained above.
In Fig. 3 the stress components are plotted along the direction $\psi=90°$ where the only parameter set at $\psi=90°$ is $a_6$ which is obtained by imposing a condition on $\sigma_{\psi\psi}$. The agreement between finite element results and theoretical stresses is very good also for the stress components not directly involved in the determination of the parameters $a_4$, $a_5$ $a_6$ and $a_7$. A slightly larger discrepancy between numerical and theoretical results is shown in Fig. 4 for the direction $\psi = -90°$. In this case the stress components present an intensity lower than in the other directions. The improvement introduced by considering the higher order terms with respect to the solution based on $K_I$, $K_{II}$ and the T-stress is evident.

| d/t | $a_1$ | $a_2$ | $a_3$ | $a_4$ | $a_5$ | $a_6$ | $a_7$ |
|---|---|---|---|---|---|---|---|
| t= 1 | MPa mm$^{0.5}$ | MPa mm$^{0.5}$ | MPa | MPa mm$^{-0.5}$ | MPa mm$^{-0.5}$ | MPa mm$^{-1}$ | MPa mm$^{-1}$ |
| 1 | - 1.73 | - 4.10 | 4.87 | - 4.02 | - 1.00 | 3.50 | 1.02 |
| | $K_I$=4.35 | $K_I$= -10.28 | T=19.5 | | | | |

Table 1: Parameters of the stress field, overlap joints

## INFLUENCE ON STRAIN ENERGY DENSITY OF HIGHER ORDER TERMS

The SED approach was later extended to thin welded lap joints [18] considering two values of the control radius, $R_0$ = 0.15 and $R_0$ = 0.28 mm.
Together with the SED values directly determined from the FE models, that paper documented also the SED values determined on the basis of the mode 1 and mode 2 NSIFs, $K_I$ and $K_{II}$, the T-stress which plays an essential role in the case of thin welded joints. The deviation values $\Delta = (\overline{W}_{K_I,K_{II},T^*} - \overline{W}_{FE}) / \overline{W}_{FE}$, showed that for the sheet thickness $t$=5 mm, the maximum deviation with respect to the FE results was 3.6% for $R_0$=0.15 mm and 3.1% for $R_0$=0.28 mm [18]. When $t$ = 1 mm, the deviation increased up to 25.0% for $R_0$=0.28 mm and up to 9.6% for $R_0$=0.15 mm (see Tab. 3). This means that in the presence of a sheet thickness $t \leq 1$ mm and $R_0$=0.28 mm, the SED depends not only $K_I$, $K_{II}$ and T-stress but also on other nonsingular stress components. The averaged SED can be easily determined directly from the FE model. Alternatively, a complex expression based on Eq (6a-c), involving the first seven terms has been derived and reported herein for sake of brevity.
A comparison between the SED from FE models and that obtained considering the parameters $a_1$, $a_2$, …$a_7$ already reported in Tab. 1, is shown in Tab. 2. The deviation values $\Delta = (\overline{W}_{HOT} - \overline{W}_{FE}) / \overline{W}_{FE}$ is less than 3%.

| $R_0$=0.28mm, ρ=0 mm t=1mm | $\overline{W}_{FE}$ (×10$^3$) (MJ/m$^3$) | $\overline{W}_{HOT}$ (×10$^3$) (MJ/m$^3$) | Δ (%) | $\overline{W}_{K_I,K_{II},T^*}$ (×10$^3$) (MJ/m$^3$) | Δ (%) |
|---|---|---|---|---|---|
| d/t=0.5 | 1.412 | 1.453 | 2.9 | 1.765 | 25.0 |
| 1 | 1.208 | 1.214 | 0.5 | 1.509 | 25.0 |
| 3 | 1.181 | 1.193 | 1.0 | 1.443 | 22.2 |

Table 2: Mean values of the strain energy density over the control volumes for welded lap joints, with F/(t×1)=10 MPa; values based on T* determined on the ligament, close to the point of singularity, r ≤ 0.03 mm.

| Δσ (MPa) | $\overline{W}_e$ x 10$^3$ (MJ/m$^3$) | $\overline{W}_p$ x 10$^3$ (MJ/m$^3$) |
|---|---|---|
| 10 | 1.120 | 1.120 |
| 20 | 4.481 | 4.485 |
| 40 | 17.93 | 18.07 |
| 80 | 71.72 | 79.68 |
| 110 | 135.5 | 171.8 |

Table 3: Mean values of SED as determined from linear elastic and elasto-plastic analyses (control volume $R_0$=0.28 mm)

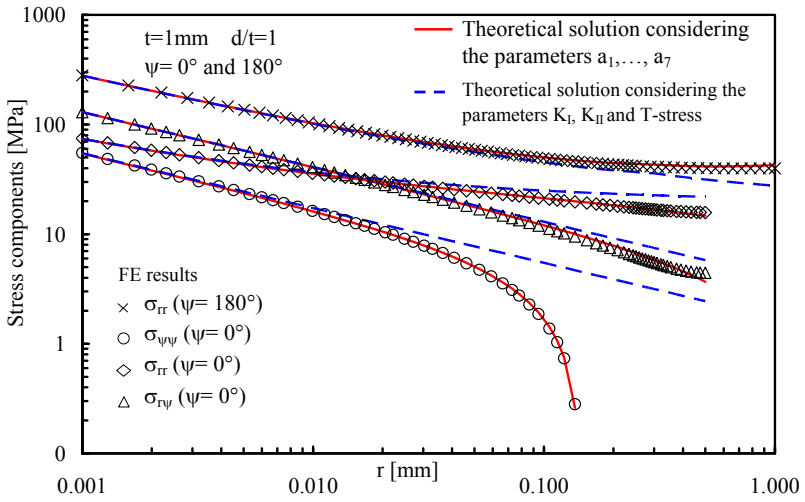


Figure 2 Stress field along the ligament line for the case d/t=1 and t=1 mm.

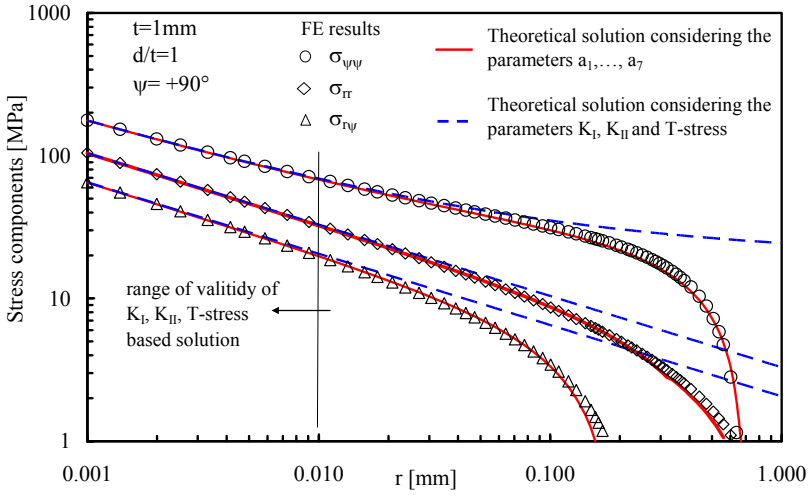


Figure 3. Stress field along the direction ψ=90° for the case d/t=1.

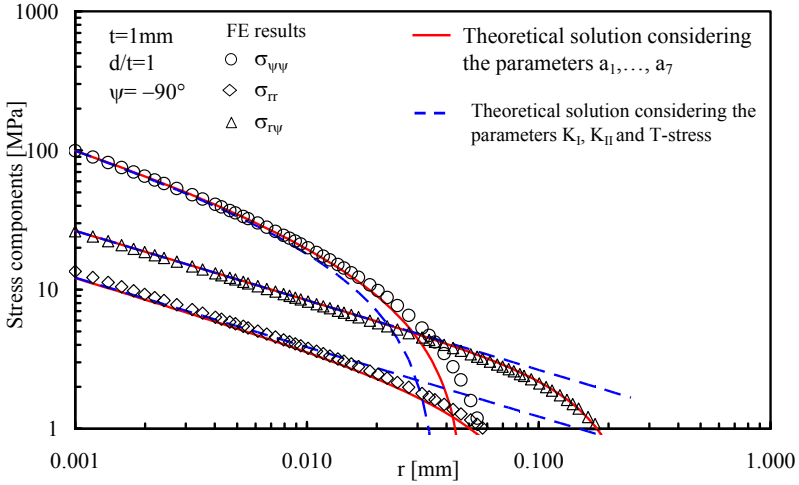


Figure 4: Stress field along the direction ψ=-90° for the case d/t=1.

## LIMITATIONS TO THE LINEAR ELASTIC APPROACH

Let us assume for the material the Ramberg-Osgood law, according to which the uniaxial tensile strain ε is related to the uniaxial stress σ according to the expression:

$$\varepsilon = \frac{\sigma}{E} + \left(\frac{\sigma}{K'}\right)^{n'} \tag{10}$$

where $1 \le n' \le \infty$. The analyses were carried out under plane strain conditions by introducing into the stress-strain curve E, K' and n'=6.66. Table 3 summarizes the values of the SED parameter as a function of the applied Δσ. It is interesting to observe that for values of $\Delta\sigma < 40$ MPa the elastic and elastic-plastic values are close each other. When Δσ=110 MPa, that is a typical value for this kind of joints at $10^5$ cycles to failure, the SED under elastic conditions is significantly different from the elastic-plastic case. The different role played by plasticity at different number of cycles can also be used as justification of the different slope shown by thin lap joints under shear loading and welded joints under tensile loading.

## CONCLUSIONS

The present investigation is aimed to present and apply a useful set of equations able to describe accurately the stress components also in those cases where the mode I and mode II stress intensity factors used in combination with the T-stress, fail to describe the complete stress field ahead the slit tip.
A practical example of a thin-thickness welded lap joint characterized by different jointing face width to thickness ratio, ranging $d/t$ from 0.5 to 3, is investigated. The stress field and the strain energy averaged over a control volume can be evaluated with satisfactory precision only taking into account further four other terms besides $K_I$, $K_{II}$ and T.

## REFERENCES

[1] M.L. Williams, J Appl Mech, 24 (1957) 109
[2] J.R. Rice, J Mech Phys Solids, 22 (1974) 17.
[3] S.G. Larsson, A.J. Carlsson, J Mech Phys Solids, 21(1973) 263.
[4] R. Gross, A. Mendelson, Int J Fract Mech, 8 (1972) 267.
[5] W. C. Carpenter, Int J Fracture, 27 (1985) 63.
[6] MR Ayatollahi MJ Pavier and DJ Smith, Int. J Fract, 91(1998) 283.
[7] Y.Z. Chen, Int J Solids and Struct, 37 (2000) 1629.
[8] T. Fett, Engng Fract Mech, 69 (2002) 69.
[9] C.J. Christopher, M.N. James, E.A. Patterson, K. F. Tee, Int J Fract, 148 (2007) 361
[10] C.J. Christopher, M.N. James, E.A. Patterson, K. F. Tee, Eng Fract Mech, 75 (2008) 4190
[11] C. Colombo, Y. Du, M.N. James, E.A.Patterson, L.Vergani, Fatigue Fract Engng Mater Struct (in press)
[12] Y.Z. Chen, X.Y. Lin, Z.X. Wang, Engng Fract Mech, 77 (2010) 753.
[13] K. Ramesh, S. Gupta and A.K. Srivastava, Int J Fract, 79 (1996) R37.
[14] K. Ramesh, S. Gupta, A.A. Kelkar, Engng Fract Mech, 56 (1997) 25.
[15] MR Ayatollahi, M. Nejati (in press), Fatigue Fract Engng Mater Struct, (available online).
[16] Q.Z. Xiao, B.L. Karihaloo and X.Y. Liu, Int J Fract, 125 (2004) 207.
[17] Q.Z. Xiao, B.L. Karihaloo, Eng. Fract. Mech., (2007) 74 1107
[18] P. Lazzarin, F. Berto, D. Radaj, Fatigue Fract. Engng. Mater. Struct., 32 (2009) 713.
[19] F. Berto, P. Lazzarin, Int J Fract, 161 (2010) 221.